NANO LETTERS

Letter

pubs.acs.org/NanoLett

One-Pot Synthesis of Protein-Embedded Metal–Organic Frameworks with Enhanced Biological Activities

Fengjiao Lyu,[†] Yifei Zhang,[†] Richard N. Zare,[‡] Jun Ge,*[,†] and Zheng Liu*[,†]

[†]Key Lab for Industrial Biocatalysis, Ministry of Education, Department of Chemical Engineering, Tsinghua University, Beijing 100084, China

[‡]Department of Chemistry, Stanford University, Stanford, California 94305-5080, United States

Supporting Information

ABSTRACT: Protein molecules were directly embedded in metal–organic frameworks (MOFs) by a coprecipitation method. The protein molecules majorly embedded on the surface region of MOFs display high biological activities. As a demonstration of the power of such materials, the resulting Cyt *c* embedded in ZIF-8 showed a 10-fold increase in peroxidase activity compared to free Cyt *c* in solution and thus gave convenient, fast, and highly sensitive detection of trace amounts of explosive organic peroxides in solution.

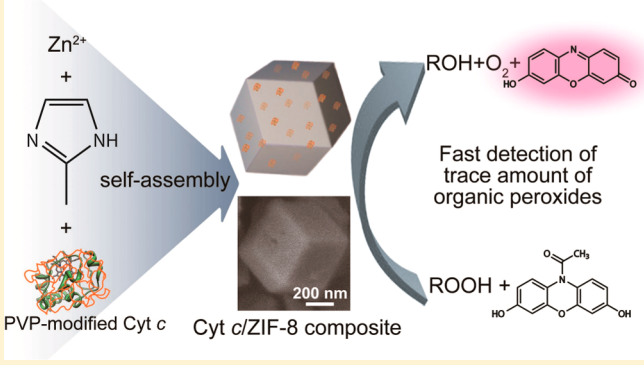

KEYWORDS: *Enzyme, metal–organic framework, nanomaterials, biocatalysis*

Metal–organic frameworks (MOFs)[1,2] hold great promise for a variety of applications including gas storage,[3,4] chemical separation,[5,6] catalysis,[7] sensing,[8] and fuel cells,[9] as well as hosting many guest species including lanthanide cations,[10] nanoparticles,[11] and dyes.[12] However, proteins, carriers of biological functions of living systems, have not yet been fully integrated with MOFs, leaving many interesting properties of the protein–MOF composite materials undiscovered. The preparation of various protein–MOF composite materials with biological functions remains a major challenge. If successful, it would greatly expand the applications of MOFs in many fields such as bioanalysis, biocatalysis, and biomedical engineering. Successful adsorption of protein molecules into presynthesized MOFs with extremely large pores has been recently reported as a way to immobilize protein onto MOFs.[13−15] However, because of the large size of protein molecules compared to the much smaller aperture of most of the common MOFs, a general method for preparation of protein-embedded MOFs is still a big challenge.

On the basis of the extensive reported studies for zeolitic imidazolate frameworks,[16] in this study we propose a new strategy that directly synthesizes protein-embedded MOFs. For the present study, cytochrome c (Cyt *c*), which has important applications in bioanalytical field,[17] was chosen as a model protein, which we attach to zeolitic imidazolate framework (ZIF-8).[18] ZIF-8 has a prototypical structure of zeolites[16] and is a representative common MOF with small pores. The versatility of this method was evaluated by using other proteins such as horseradish peroxidase (HRP) and lipase and using other MOF scaffolds such as ZIF-10. Furthermore, we demonstrated that the Cyt *c*-embedded MOF can be applied in the fast and highly sensitive detection of explosive organic peroxides, which are frequently used in liquid bombs.

In a typical experiment, a solution (50 μL) containing both Cyt *c* (50 mg/mL) and polyvinylpyrrolidone (PVP) (15 mg/mL) was added to a methanol solution of zinc nitrate hexahydrate (25 mM, 50 mL) and 2-methylimidazole (25 mM, 50 mL) (Figure 1). PVP was utilized to assist the dispersion and stabilization of the protein in methanol. The growth of ZIF-8 crystal was observed by transmission electron

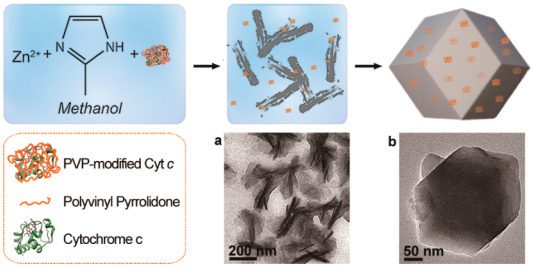

Figure 1. Preparation of the cytochrome *c*-embedded ZIF-8. A schematic showing the synthesis of the Cyt *c*/ZIF-8 composite. TEM images of the Cyt *c*/ZIF-8 composite obtained after a reaction time of 5 min (a) and 24 h (b).

Received: July 12, 2014
Revised: September 4, 2014
Published: September 11, 2014

   dx.doi.org/10.1021/nl5026419 | *Nano Lett.* 2014, 14, 5761–5765

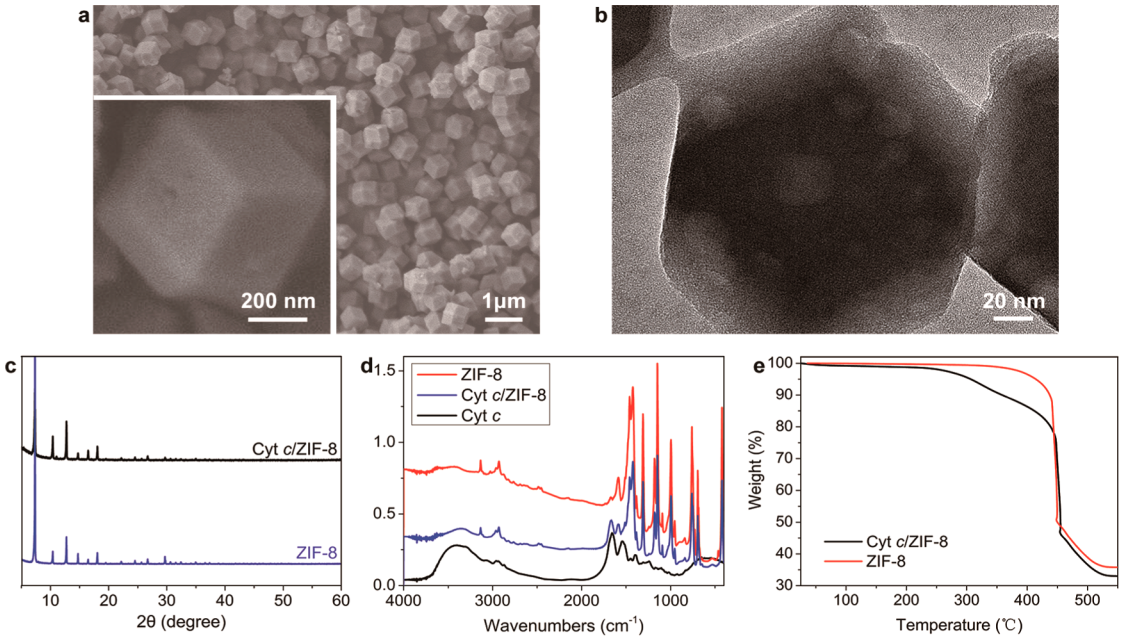

Figure 2. (a) SEM image of the Cyt *c*/ZIF-8 composite. (b) TEM image of the negatively stained Cyt *c*/ZIF-8 composite. (c) XRD patterns of ZIF-8 and the Cyt *c*/ZIF-8 composite. (d) FTIR spectra of pure ZIF-8 crystal, the Cyt *c*/ZIF-8 composite, and Cyt *c*. (e) TGA curves of ZIF-8 and the Cyt *c*/ZIF-8 composite in air.

microscopy (TEM), which showed that Zn^{2+} and 2-methylimidazole first assembled into rods (Figure 1a) and then formed rhombic dodecahedron crystals after 24 h (Figure 1b).

The scanning electron microscope (SEM) images reveal that the synthesized Cyt *c*/ZIF-8 composite displays the same morphology as pure ZIF-8 (Figures 2a and S1, Supporting Information). The X-ray diffraction (XRD) pattern of Cyt *c*/ZIF-8 composite also agrees well with that of pure ZIF-8 (Figure 2c). Under TEM, after the sample is negatively stained with phosphotungstic acid, the image of Cyt *c*/ZIF-8 composite (Figure 2b) shows light spots (from 5 to 25 nm), which cannot be observed in negatively stained pure ZIF-8 (Figure S2, Supporting Information). The light spots resulted from the low electron-scattering density of Cyt *c* molecules and their aggregates contained in MOFs. The Fourier transform infrared spectroscopy (FTIR) of the powders of pure ZIF-8 crystal, Cyt *c*, and Cyt *c*/ZIF-8 composite are shown in Figure 2d. The signal at 1664 cm^{-1} corresponding to the stretching modes of double bonds and carbonyls in Cyt *c*[19] appears in the composite, suggesting the existence of Cyt *c*. The thermal gravimetric analysis (TGA) in air (Figure 2e) also confirms the presence of Cyt *c* in the composite. The first-stage decomposition of the Cyt *c*/ZIF-8 composite in air starts from 250 °C and finishes around 350 °C, being much lower than that of the pure ZIF-8 crystal (450 °C). About 10% of weight loss occurs during the first stage, which is attributed to the decomposition of the protein/PVP complex. Determined by inductively coupled plasma mass spectrometry (ICP−MS), the content of Fe in the pure ZIF-8, Cyt *c*/ZIF-8 composite, and pure Cyt *c* was 43.2, 335.4, and 3648.0 μg/g, respectively (Table S1, Supporting Information). As there is one equiv of Fe per protein, it is calculated that the weight percentage of Cyt *c* in ZIF-8 is around 8%, which agrees well with the results of protein BCA measurement and TGA analysis.

To investigate whether the Cyt *c* molecules are just adsorbed on the surface of ZIF-8 or are embedded within ZIF-8, a calcination process at 325 °C for 2 h was carried out to remove protein molecules from the composite (the temperature was chosen based on the thermal gravimetric analysis). The TEM and SEM images of Cyt *c*/ZIF-8 composite after calcination show the existence of small cavities with a size ranging from 5 to 20 nm (Figure 3a,c), which is resulted from the removal of

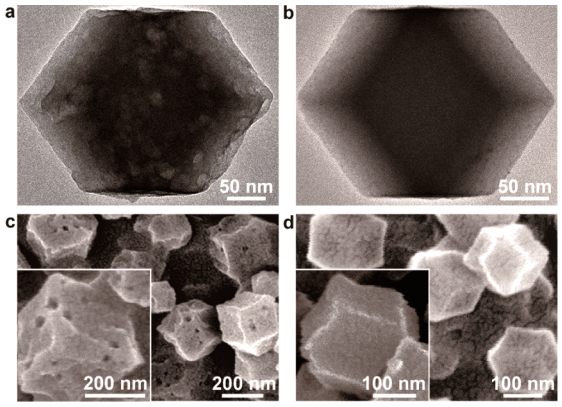

Figure 3. TEM images of calcinated Cyt *c*/ZIF-8 composite (a) and calcinated pure ZIF-8 crystal (b). SEM images of calcinated Cyt *c*/ZIF-8 composite (c) and calcinated pure ZIF-8 crystal (d).

Cyt *c* molecules and their aggregates. In contrast, such pores do not appear in the pure ZIF-8 crystal after the same calcination treatment (Figure 3b,d). Especially from SEM image (Figure 3c), we can identify that most protein molecules are embedded on the surface region of ZIF-8 crystals.

The nitrogen sorption study was performed on ZIF-8, Cyt *c*/ZIF-8 composite, and the calcinated products (Figure S3, Supporting Information). The distribution of micropores calculated by the Saito−Foley method (SF method) (Figure S4, Supporting Information) revealed that when Cyt *c* was embedded in ZIF-8 the MOF scaffold of the composite has the

dx.doi.org/10.1021/nl5026419 | *Nano Lett.* 2014, 14, 5761−5765

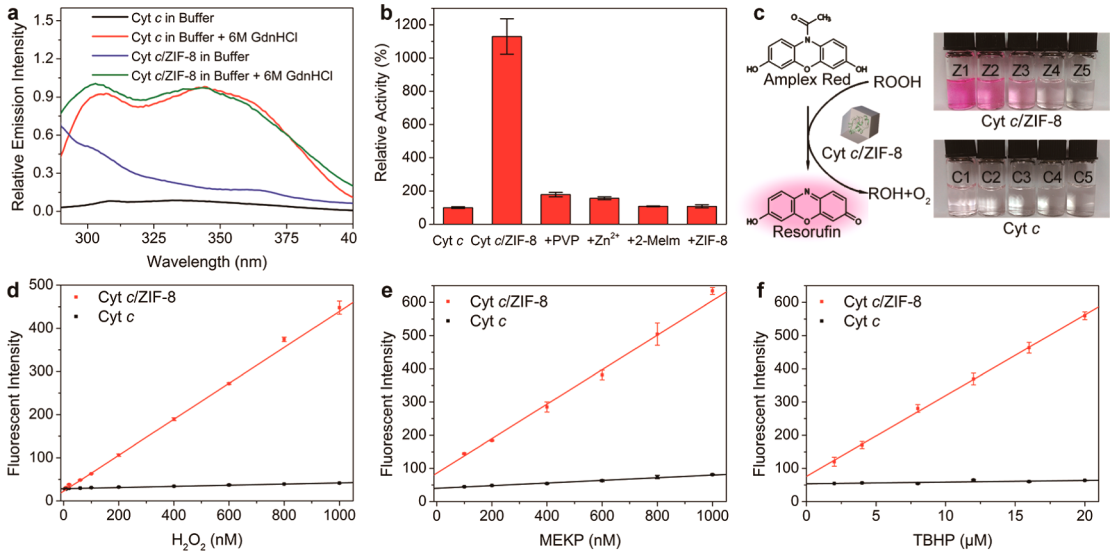

Figure 4. (a) Fluorescence spectra of Cyt *c*, Cyt *c* denatured by GdnHCl, Cyt *c*/ZIF-8 composite, and Cyt *c*/ZIF-8 composite denatured by GdnHCl. (b) The relative peroxidase activity of Cyt *c*, Cyt *c* /ZIF-8 composite, PVP/Cyt *c* mixture, Cyt *c*/zinc ion mixture, Cyt *c*/2-methylimidazole mixture, and Cyt *c*/ZIF-8 mixture. All the enzymatic assays were carried out at the same protein concentration, with the activity of free Cyt *c* in solution as 100%. (c) Schematic showing the detection of H_2O_2. Photographs showing visible detection of H_2O_2. For Z1−Z5, Cyt *c*/ZIF-8 composite was used, while for C1−C5, free Cyt *c* was used as the biocatalyst. In all detections, the concentration of Cyt *c* and Amplex Red were maintained at 2 and 100 μM, respectively. From Z1−Z5 and C1−C5, the concentrations of H_2O_2 in the Tris-HCl buffer pH 7.4 are 80, 40, 20, 10, and 0 μM, respectively. Photographs were taken 2 min after mixing all the protein samples and substrates. Linear relationships between the fluorescence intensity and the concentration of H_2O_2 (d), MEKP (e), and TBHP (f), with the catalysis of Cyt *c*/ZIF-8 composite and free Cyt *c*.

same micropore structure compared to pure ZIF-8. Even the removal of embedded protein molecules by calcination did not affect the MOF scaffold structure. This indicates that the embedded protein molecules have no influence on the crystal growth of ZIF-8. However, when we further calculated the pore size distribution of the above calcinated products using the Barrett−Joyner−Halenda adsorption method (BJH method) (Figure S5, Supporting Information), the calcinated Cyt *c*/ZIF-8 composite showed an increase in the pores around 15−35 nm, consistent with the SEM result (Figure 3c), which is due to the removal of embedded protein molecules and aggregates. The above study led us to the mechanism of the formation of Cyt *c*/ZIF-8 composite. Without using PVP as additive to help the dispersion of Cyt *c* in methanol, we synthesized the Cyt *c*/ZIF-8 composite (Figure S6a, Supporting Information) (Cyt *c* was dispersed in methanol by a harsh probe sonication). After calcination of the Cyt *c*/ZIF-8 composite without polymer additives, small cavities with sizes ranging from 5 to 20 nm appeared (Figure S6b, Supporting Information), which resulted from the removal of Cyt *c* molecules. The successful preparation of Cyt *c*/ZIF-8 composite without using PVP suggests that it is probably the coordinating interaction between Zn^{2+} and amide bonds of protein that helps the embedment of Cyt *c* in ZIF-8 during crystal growth.

The protein configuration of Cyt *c* embedded in ZIF-8 was examined with steady-state fluorescence spectroscopy and compared to its native counterpart in solution.[20] It is noted here the heme group nearly completely quenches the emission spectrum of Cyt *c* in its native state in phosphate buffer (50 mM, pH 7.0) (Figure 4a), due to the Trp-59 residue that is located ∼5 Å from the heme edge.[14] Once 6 M guanidine hydrochloride (GdnHCl) was added, Cyt *c* was unfolded, and the maximum emission centered at 307 and 344 nm appears (Figure 4a) arising from the exposure of tyrosine and tryptophan residues.[21] The Cyt *c*/ZIF-8 composite in phosphate buffer solution displays no emission peak at 300−400 nm (Figure 4a), as does its native counterpart. Once exposed to GdnHCl, the Cyt *c*/ZIF-8 composite shows again a similar emission spectrum to that of free Cyt *c*. This result indicates that the Cyt *c* embedded in ZIF-8 highly preserves its native configuration, the same as its free form in solution.

The specific activity of the Cyt *c* embedded in ZIF-8 was determined by a standard method[22] using hydrogen peroxide (H_2O_2) (2 mM) and 2,2′-azinobis(2-ethylbenzthiazoline-6-sulfonate) (ABTS) (532 μM) as the substrates under saturated conditions in potassium phosphate buffer (50 mM, pH 7.0). Before the enzymatic assay, the weight percentage of protein in the Cyt c-MOF was measured as ∼10% by a standard BCA protein assay kit, which agrees well with the TGA and ICP−MS analysis. The encapsulation yield of Cyt *c* during the coprecipiation process was calculated as 82.3%. As shown in Figure 4b, at the same protein concentration, the embedded Cyt *c* showed a 10-fold increase in activity compared to the free Cyt *c* in solution. The control experiments showed that the presence of PVP and Zn^{2+} in solution only increased the activity of Cyt *c* by 79% and 57%, respectively, and that the presence of 2-methylimidazole or ZIF-8 in solution had no effect on the activity of Cyt *c* (Figure 4b). Moreover, pure ZIF-8 itself had no catalytic activity toward the substrates. Especially, the mixture of Cyt *c* and ZIF-8 has almost the same activity compared to free Cyt *c* (the last column in Figure 4b), indicating that the embedment of Cyt *c* in ZIF-8 must play a crucial role in the enhancement of activity.

Activity loss often occurred in enzyme immobilization or encapsulation, which is caused by either denaturation of the enzyme or hindered mass transfer within the solid carriers.[23] It is shown by silica nanospheres,[24] single enzyme nanoparticles[25] and nanogels,[26] mesoporous silica,[27] and enzyme−inorganic hybrid nanoflowers[28] that a nanoscale matrix offers a way to reduce mass transfer distance and thus enables the immobilized

dx.doi.org/10.1021/nl5026419 | *Nano Lett.* 2014, 14, 5761−5765

enzyme to display a similar activity as its native counterpart. For example, mesoporous silica has been well studied for the immobilization of Cyt *c*. About 60% to 90% of the activity of Cyt *c* immobilized on a mesoporous silica material can be retained.[29] In our study, to explore the mechanism underpinning the 10-fold increase in the apparent activity of the Cyt *c* in ZIF-8, we determined the enzymatic Michaelis–Menten kinetics of Cyt *c* in ZIF-8 with respect to H_2O_2 concentration (Figure S7, Supporting Information). We find that the embedded Cyt *c* shows a K_m value of 2 mM and a V_{max} value of 200 μM/min, whereas the K_m and V_{max} of free Cyt *c* is 15 mM and 80 μM/min, respectively. Here the significantly decreased K_m of H_2O_2, which is the substrate that needs to be directly bound to the active site of Cyt *c*,[30,31] suggests a possibility that the immobilized Cyt *c* has a higher substrate affinity toward H_2O_2 molecules. The increased substrate affinity is possibly due to the incubation of Cyt *c* in methanol, which makes a conformational change of the protein (Figure S8a, Supporting Information) to expose its heme group.[32] In addition, the microenvironment created by the immobilization carrier, ZIF-8, might also contribute to the increased substrate affinity. As reported by many previous studies,[33−35] immobilization carriers can significantly affect enzyme activity by creating microenvironments that are suitable for enzyme catalysis, resulting in a decreased apparent K_m in some cases. The increased V_{max}, however, suggests the possible contribution of the interaction between the embedded Cyt *c* and Zn^{2+} in ZIF-8 crystals to the enhancement of the catalytic activity of Cyt *c*, which is also observed when incubating free Cyt *c* with free Zn^{2+} in solution (Figure 4b). Such effect of metal ions in crystals on enzymatic activity was also reported by our previous study[28] and others.[36] On the basis of the enzymatic kinetics, we proposed the above mechanism, which remains hypothetical and will require further experiments to confirm.

Using the same method, we prepared horseradish peroxidase (HRP)/ZIF-8, lipase (from *Thermomyces lanuginosus*)/ZIF-8, and Cyt *c*/ZIF-10 composites (SEM images, Figures S9–S11, Supporting Information). The activities of HRP, lipase in ZIF-8, and Cyt *c* in ZIF-10 were determined to be ~28%, ~88%, and ~87% (Figure S12, Supporting Information), respectively, compared to the free enzyme in solution. During the preparation of enzyme/MOF composites, when incubated in methanol, Cyt *c* showed an increased activity up to 311%. After preparation of the Cyt *c*/ZIF-8 composite, a much higher activity (~1130%) can be observed arising from the activation effect of ZIF-8. For horseradish peroxidase and lipase incubated in methanol, a blue shift and increased fluorescent intensity was observed in the fluorescence spectrum (Figure S8b,c, Supporting Information), indicating a conformational change of protein in methanol. Consistent with the conformational change, horseradish peroxidase and lipase were measured to be deactivated in methanol, with only 8% and 15% of activity retained, respectively. After preparation of the enzyme/ZIF-8 composites, the activity was further increased to 28% and 88% for horseradish peroxidase and lipase, respectively. Thus, the activation effect of ZIF-8 was observed for these three different proteins, though at different levels. For Cyt *c*/ZIF-10 composite, the retention of only ~87% activity is possibly due to the inhibition effect of imidazole[37] used for the synthesis of ZIF-10.

Peroxide-based explosives are used in criminal and terrorist activities, which demands a facile, rapid, and sensitive determination of the explosive organic peroxides in solution.[38] The excellent peroxidase activity of the Cyt *c*/ZIF-8 leads us to evaluate its potential in the detection of hydrogen peroxide (H_2O_2), methyl ethyl ketone peroxide (MEKP), and *tert*-butyl hydroperoxide (TBHP) in solution. Using these above peroxides and *N*-acetyl-3,7-dihydroxyphenoxazine (Amplex Red)[39] as the substrates, the Cyt *c*-catalyzed oxidation of Amplex Red produces resorufin, which is fluorescently detectable (Figure 4c). In a typical detection of H_2O_2, the fluorescence of resorufin was measured 2 min after incubating Amplex Red (5 μM), Cyt *c*/ZIF-8 composite (2 μM of protein), and H_2O_2 in Tris-HCl buffer (50 mM, pH 7.4) at room temperature. As shown in Figure 4d, a good linearity between the intensity of fluorescence and the concentration of H_2O_2 in the range of 5 nM to 1 μM is obtained. The detection limit is 3 nM at a signal-to-noise ratio of 3, which is the lowest detection limit compared to the reported ones.[40−43] In comparison, free Cyt *c* (at the same protein concentration) as a control gave a much slower reaction rate, resulting in no detectable signals, while the ZIF-8 itself has no catalytic activity. The determinations of MEKP and TBHP using Cyt *c*/ZIF-8 as the catalyst also showed good linearity and sensitivity (Figures 4e,f) in the range of 100 nM to 1 μM and 2 μM to 20 μM, respectively. In contrast, free Cyt *c* (at the same protein concentration) as a control did not produce detectable signals for the detection of MEKP and TBHP in solution. At high concentrations of Amplex Red (100 μM) and H_2O_2 (10–80 μM), the Cyt *c*/ZIF-8 composite (2 μM of protein) allows fast, visible detection of H_2O_2 within 2 min, whereas the free Cyt *c* fails to respond (Figure 4c).

In conclusion, we report a facile method for the direct synthesis of protein-embedded MOFs with biological activity. The generality of this method was validated by loading cytochrome *c*, horseradish peroxidase, and lipase, onto ZIF-8 and ZIF-10. The apparent activity of Cyt *c* in ZIF-8 was increased by 10-fold, compared to its native counterpart in solution. Rapid, sensitive, visible detection of highly explosive organic peroxides was achieved using the Cyt *c*-MOF composite. Given the variety of proteins and the ever-expanding pool of MOFs, this new method for the preparation of protein–MOF composites opens avenues for combining together their properties and functionalities, thereby displaying novel important features enabling new applications in biosensors, analytical devices, biofuel cells, and industrial biocatalysis.

■ ASSOCIATED CONTENT

Ⓢ Supporting Information

Experimental details for the synthesis of protein–MOF composites, SEM, TEM, and BET characterizations, and measurements of enzymatic activities. This material is available free of charge via the Internet at http://pubs.acs.org.

■ AUTHOR INFORMATION

Corresponding Authors

*(J.G.) E-mail: junge@mail.tsinghua.edu.cn.
*(Z.L.) E-mail: liuzheng@mail.tsinghua.edu.cn.

Notes

The authors declare no competing financial interest.

■ ACKNOWLEDGMENTS

This work was supported by the National High Technology Research and Development Program ("863" Program) of

China under the grant number of 2014AA020507, the National Natural Science Foundation of China under the grant numbers 21036003 and 21206082, and the Tsinghua University Initiative Scientific Research Program under the grant number of 20131089191.

REFERENCES

(1) Furukawa, H.; Cordova, K. E.; O'Keeffe, M.; Yaghi, O. M. *Science* **2013**, *341*, 1284−1293.
(2) Yaghi, O. M.; O'Keeffe, M.; Ockwig, N. W.; Chae, H. K.; Eddaoudi, M.; Kim, J. *Nature* **2003**, *423*, 705−714.
(3) Klontzas, E.; Mavrandonakis, A.; Tylianakis, E.; Froudakis, G. E. *Nano Lett.* **2008**, *8*, 1572−1576.
(4) Morris, R. E.; Wheatley, P. S. *Angew. Chem., Int. Ed.* **2008**, *47*, 4966−4981.
(5) Maes, M.; Alaerts, L.; Vermoortele, F.; Ameloot, R.; Couck, S.; Finsy, V.; Denayer, J. F. M.; De Vos, D. E. *J. Am. Chem. Soc.* **2010**, *132*, 2284−2292.
(6) Song, Q.; Nataraj, S. K.; Roussenova, M. V.; Tan, J. C.; Hughes, D. J.; Li, W.; Bourgoin, P.; Alam, M. A.; Cheetham, A. K.; Al-Muhtaseb, S. A.; Sivaniah, E. *Energy Environ. Sci.* **2012**, *5*, 8359−8369.
(7) Lee, J.; Farha, O. K.; Roberts, J.; Scheidt, K. A.; Nguyen, S. T.; Hupp, J. T. *Chem. Soc. Rev.* **2009**, *38*, 1450−1459.
(8) Chen, B.; Xiang, S.; Qian, G. *Acc. Chem. Res.* **2010**, *43*, 1115−1124.
(9) Proietti, E.; Jaouen, F.; Lefèvre, M.; Larouche, N.; Tian, J.; Herranz, J.; Dodelet, J.-P. *Nat. Commun.* **2011**, *2*, 416.
(10) An, J.; Shade, C. M.; Chengelis-Czegan, D. A.; Petoud, S.; Rosi, N. L. *J. Am. Chem. Soc.* **2011**, *133*, 1220−1223.
(11) Buso, D.; Jasieniak, J.; Lay, M. D. H.; Schiavuta, P.; Scopece, P.; Laird, J.; Amenitsch, H.; Hill, A. J.; Falcaro, P. *Small* **2012**, *8*, 80−88.
(12) Sun, C.-Y.; Wang, X.-L.; Zhang, X.; Qin, C.; Li, P.; Su, Z.-M.; Zhu, D.-X.; Shan, G.-G.; Shao, K.-Z.; Wu, H.; Li, J. *Nat. Commun.* **2013**, *4*, 2717.
(13) Deng, H.; Grunder, S.; Cordova, K. E.; Valente, C.; Furukawa, H.; Hmadeh, M.; Gándara, F.; Whalley, A. C.; Liu, Z.; Asahina, S.; Kazumori, H.; O'Keeffe, M.; Terasaki, O.; Stoddart, J. F.; Yaghi, O. M. *Science* **2012**, *336*, 1018−1023.
(14) Chen, Y.; Lykourinou, V.; Vetromile, C.; Hoang, T.; Ming, L.-J.; Larsen, R. W.; Ma, S. *J. Am. Chem. Soc.* **2012**, *134*, 13188−13191.
(15) Lykourinou, V.; Chen, Y.; Wang, X.-S.; Meng, L.; Hoang, T.; Ming, L.-J.; Musselman, R. L.; Ma, S. *J. Am. Chem. Soc.* **2011**, *133*, 10382−10385.
(16) Park, K. S.; Ni, Z.; Côté, A. P.; Choi, J. Y.; Huang, R.; Uribe-Romo, F. J.; Chae, H. K.; O'Keeffe, M.; Yaghi, O. M. *Proc. Natl. Acad. Sci. U.S.A.* **2006**, *103*, 10186−10191.
(17) Qu, L.-L.; Li, D.-W.; Qin, L.-X.; Mu, J.; Fossey, J. S.; Long, Y.-T. *Anal. Chem.* **2013**, *85*, 9549−9555.
(18) Hayashi, H.; Côté, A. P.; Furukawa, H.; O'Keeffe, M.; Yaghi, O. M. *Nat. Mater.* **2007**, *6*, 501−506.
(19) Schlereth, D. D.; Mäntele, W. *Biochemistry* **1993**, *32*, 1118−1126.
(20) Timperman, A. T.; Oldenburg, K. E.; Sweedler, J. V. *Anal. Chem.* **1995**, *67*, 3421−3426.
(21) Pajot, P. *Eur. J. Biochem.* **1976**, *63*, 263−269.
(22) Ozgen, M.; Reese, R. N.; Tulio, A. Z.; Scheerens, J. C.; Miller, A. R. *J. Agric. Food Chem.* **2006**, *54*, 1151−1157.
(23) Cao, L.; van Langen, L.; Sheldon, R. A. *Curr. Opin. Biotechnol.* **2003**, *14*, 387−394.
(24) Luckarift, H. R.; Spain, J. C.; Naik, R. R.; Stone, M. O. *Nat. Biotechnol.* **2004**, *22*, 211−213.
(25) Kim, J.; Grate, J. W. *Nano Lett.* **2003**, *3*, 1219−1222.
(26) Yan, M.; Ge, J.; Liu, Z.; Ouyang, P. *J. Am. Chem. Soc.* **2006**, *128*, 11008−11009.
(27) Lei, C.; Shin, Y.; Liu, J.; Ackerman, E. J. *J. Am. Chem. Soc.* **2002**, *124*, 11242−11243.
(28) Ge, J.; Lei, J.; Zare, R. N. *Nat. Nanotechnol.* **2012**, *7*, 428−432.
(29) Kao, K.-C.; Lee, C.-H.; Lin, T.-S.; Mou, C.-Y. *J. Mater. Chem.* **2010**, *20*, 4653−4662.
(30) Lee, C.-H.; Lang, J.; Yen, C.-W.; Shih, P.-C.; Lin, T.-S.; Mou, C.-Y. *J. Phys. Chem. B* **2005**, *109*, 12277−12286.
(31) Silaghi-Dumitrescu, R.; Cooper, C. E. *Dalton Trans.* **2005**, 3477−3482.
(32) Yang, X.; Zhao, C.; Ju, E.; Ren, J.; Qu, X. *Chem. Commun.* **2013**, *49*, 8611−8613.
(33) Mateo, C.; Palomo, J. M.; Fernandez-Lorente, G.; Guisan, J. M.; Fernandez-Lafuente, R. *Enzyme Microb. Technol.* **2007**, *40*, 1451−1463.
(34) Kim, J.; Grate, J. W.; Wang, P. *Trends Biotechnol.* **2008**, *26*, 639−646.
(35) Simard, J. M.; Szymanski, B.; Rotello, V. M. *Med. Chem.* **2005**, *1*, 153−157.
(36) Wang, L.-B.; Wang, Y.-C.; He, R.; Zhuang, A.; Wang, X.; Zeng, J.; Hou, J. G. *J. Am. Chem. Soc.* **2013**, *135*, 1272−1275.
(37) Kokhan, O.; Shinkarev, V. P.; Wraight, C. A. *J. Biol. Chem.* **2010**, *285*, 22513−22521.
(38) Burks, R. M.; Hage, D. S. *Anal. Bioanal. Chem.* **2009**, *395*, 301−313.
(39) Zhou, M.; Diwu, Z.; Panchuk-Voloshina, N.; Haugland, R. P. *Anal. Biochem.* **1997**, *253*, 162−168.
(40) Sanford, A. L.; Morton, S. W.; Whitehouse, K. L.; Oara, H. M.; Lugo-Morales, L. Z.; Roberts, J. G.; Sombers, L. A. *Anal. Chem.* **2010**, *82*, 5205−5210.
(41) Chen, W.; Cai, S.; Ren, Q.-Q.; Wen, W.; Zhao, Y.-D. *Analyst* **2012**, *137*, 49−58.
(42) Wen, F.; Dong, Y.; Feng, L.; Wang, S.; Zhang, S.; Zhang, X. *Anal. Chem.* **2011**, *83*, 1193−1196.
(43) Watabe, S.; Sakamoto, Y.; Morikawa, M.; Okada, R.; Miura, T.; Ito, E. *PLoS One* **2011**, *6*, e22955.